Available online at www.sciencedirect.com
SCIENCE DIRECT
Journal of Catalysis 228 (2004) 333–346
JOURNAL OF CATALYSIS
www.elsevier.com/locate/jcat

Synthesis, characterization, and catalytic activity of vanadium-incorporated, -grafted, and -immobilized mesoporous MCM-41 in the oxidation of aromatics

S. Shylesh, A.P. Singh *

Catalysis Division, National Chemical Laboratory, Pune 411 008, India

Received 15 June 2004; revised 10 August 2004; accepted 31 August 2004
Available online 22 October 2004

Abstract

Vanadium containing mesoporous molecular sieves synthesized by direct hydrothermal (V-MCM-41), grafting (V/MCM-41), and immobilization methods (V–NH_2-MCM-41) has been studied in the one-step liquid-phase oxidation of naphthalene using aqueous H_2O_2 and TBHP as oxidants. The nature of vanadium species and its interaction with the support, MCM-41, were probed in detail by XRD, FTIR, BET surface area, N_2 sorption isotherms, UV–VIS, TPR, TG-DTG, ^{13}C CP MAS NMR, SEM, and TEM. XRD, FTIR, and N_2 sorption results show that the characteristic structural features of MCM-41 are preserved after vanadia incorporation and surface modifications. Spectroscopic measurements reveal that vanadium exists mainly in tetrahedral positions for V-MCM-41 catalysts while with the grafting method the vanadium species exist as higher coordinated species and the immobilized catalyst shows that even slight changes in pretreatment conditions can change the oxidation state of vanadium ions. H_2-TPR measurements reveal that V-MCM-41 samples are reduced easily than the samples prepared by postsynthesis methods and thus point to the formation of nonreducible species in the grafted catalyst systems. Reaction data showed that the activity of the catalyst in oxidation reaction is greater at higher reaction temperatures and polar aprotic solvents promote the reaction drastically. The progressive activity of the V-MCM-41 than V/MCM-41 catalyst may be due to the presence of tetrahedral-coordinated vanadium ions in the framework positions compared to the V–O–V bond formed for V/MCM-41 and the observed higher catalytic behavior of the V–NH_2-MCM-41 catalysts may result from active metal site isolations. The difference in the selectivity behavior of as-synthesized and calcined V/MCM-41 samples shows that apart from the active redox sites, the nature of hydrophilic–hydrophobic interactions also plays an important role in selective oxidation reactions.

Keywords: Vanadium; MCM-41; Naphthalene; Oxidation; Heterogenity

1. Introduction

Molecular sieves with transition metals incorporated into the framework or impregnated/grafted and immobilized ones have attracted great interest in catalytic oxidation processes, especially in fine chemical synthesis [1–4]. Mesoporous MCM-41 having large surface areas, variable pore diameters, and high-density surface silanol sites provides the anchoring of valuable homogeneous catalysts/active organic moieties or the incorporation of redox metal ions into framework positions in a quite simple way [5] and thus enhances their intrinsic catalytic activity due to the amorphous nature of the pore walls. However, the nature of interaction and the active site isolation are entirely different in the three preparation procedures and hence a careful investigation is needed in order to account for the observed catalytic activity behavior and thereby to design a potential catalyst for a definite reaction.

Vanadium containing zeolitic molecular sieves and mesoporous materials was found to be active in a number of liquid-phase oxidation reactions using H_2O_2 as an oxidant [6–8]. A comparison of metal-incorporated zeolitic molecu-

* Corresponding author. Fax: +91-2025893761.
E-mail address: apsingh@cata.ncl.res.in (A.P. Singh).

0021-9517/$ – see front matter
doi:10.1016/j.jcat.2004.08.037

lar sieves with mesoporous materials shows that the activity and heterogenity of the zeolitic catalysts are far greater than the mesoporous sieves and these discrepancies result from active metal site isolations in which all framework metal sites are theoretically accessible for the substrate molecules and oxidant in case of zeolites. However, the pore architecture of zeolites (2–20 Å) limits the transformation of bulkier organic molecules and hence M41S materials having large pore sizes (20–100 Å) receive wide utility in various catalytic applications. But for selective hydroxylation reactions, the presence of high-density surface silanol groups contributing to the hydrophilic nature of the catalysts is not adequate for the formation of selective hydroxylated products where the formed products are more susceptible to oxidation than the reactants as in benzene/naphthalene hydroxylation. Hence the presence of high-density surface silanol groups contributing to the hydrophilic nature of the mesoporous materials must be decreased for the selective formation of oxidized products.

Even though the literature shows a broad spectrum of vanadium-incorporated (V-MCM-41) mesoporous molecular sieves [9–13], serious drawbacks of this procedure lie in the way that, the amount of metal incorporated by this procedure is low and since the active metal sites are well buried inside the pore channels, a large part of the metal sites behave as inactive species for a particular reaction. On the contrary, impregnation/grafting methods help to achieve a high percentage of metal loading and also help to disperse the active metal sites by suitably tuning the preparation procedures. However, the drawbacks are as follows:

(i) it is difficult to control the dispersity of the grafted metal species, so tiny metal oxide species can form preferentially even at relatively low concentrations,
(ii) structural collapse of the mesoporous materials occurs after high-temperature calcinations and after a particular amount of metal loading,
(iii) even though the redox properties are similar to that of an incorporated catalyst, their catalytic performance seems to be the least, and
(iv) the inherent leaching problem causes confusion on the heterogeneity of the impregnated catalysts.

But a suitable choice of the dispersing medium (solvent) and a careful tuning of the preparation procedure help to disperse the active metal species without formation of undesired tiny oxide species and hence receive considerable research and refinements. Recently, Mou et al. [14] have shown that a vanadium-immobilized catalyst is more active and selective than a V-MCM-41 catalyst in the benzene hydroxylation reaction, since for the former the active metal sites are well isolated and anchored on a suitable support and thus the leaching problem can also be minimized.

In the present study, in order to understand the role model of vanadium in various environments on mesoporous supports and how these properties influence catalytic activity and selectivity, a series of vanadium-incorporated ordered mesoporous silica (V-OMS) catalysts are synthesized and compared with vanadium-grafted and vanadium-immobilized mesoporous molecular sieves. Moreover, the present study addresses the hydrophilic–hydrophobic interactions and the nature of solvent/oxidizing agent on the heterogenity and thereby design a true heterogeneous catalyst for a specific reaction.

2. Experimental

Vanadium-incorporated molecular sieves and siliceous MCM-41 were synthesized hydrothermally in the temperature range of 100 °C, whereas vanadium-immobilized V–NH_2-MCM-41 was prepared by the organo-functionalization of Si-MCM-41 with 3-aminopropyltrimethoxysilane (3-APTS, Lancaster) and its subsequent complexation with vanadyl sulfate ($VOSO_4{\cdot}3H_2O$, Aldrich) solution, while the V/MCM-41 catalysts were prepared by the grafting of Si-MCM-41 with an alcoholic solution of $VO(acac)_2$ salt (Aldrich).

2.1. Synthesis procedure

Pure siliceous MCM-41 was synthesized from a gel having a molar composition

$$SiO_2{:}0.39Na_2O{:}0.48CTMABr{:}0.29H_2SO_4{:}100H_2O,$$

where CTMABr is cetyl trimethyl ammonium bromide (Aldrich) [15]. The gel mixture was stirred for 2 h and finally the mixture was transferred into a Teflon-lined autoclave and kept at 100 °C under static conditions for 72 h. The solid material obtained was then filtered and washed well with copious amounts of water, till the filtrate shows a neutral pH and was then air-dried. The surfactant inside the pores of the mesoporous material was removed by calcination at 540 °C for 6 h, at a heating ramp of 1 °C/min.

For the incorporation of vanadium into the framework position of MCM-41, a synthesis procedure similar to [16] was opted with minor modifications. The molar compositions of the gel mixture is

$$SiO_2{:}x\,VO_2{:}0.17Na_2O{:}0.5CTMABr{:}60H_2O,$$

where x varies from 0.018 to 0.008, and were prepared by the addition of cetyl trimethyl ammonium bromide and vanadyl sulfate to a stirred solution mixture of fumed silica under alkaline conditions. The mixture was then stirred at room temperature for 5 h and was then subsequently autoclaved at 100 °C for 4 days. For comparison, a silica polymorph was also prepared by the same method but without the addition of vanadyl sulfate solution. The obtained material was washed with water and acetone, dried at 80 °C, and finally calcined in air at 540 °C for 5 h. In order to evaluate the hydrophobicity of the material, V-MCM-41 (Si/V = 55) catalyst was silylated under nitrogen atmosphere using

dimethyldichorosilane (DMDS, Aldrich) as the silylating agent. Typically, 1 g of calcined sample was stirred in 50 ml of toluene, followed by the dropwise addition of 1 g of DMDS in toluene. The solution was then allowed to reflux for 6 h and finally the materials were filtered, washed well with toluene and acetone, and then dried at 80 °C for 3 h.

The grafting of vanadyl acetylacetonate on the mesoporous support was carried out by stirring 1 g of the support (dried at 100 °C/2 h) in an alcholic solution of $VO(acac)_2$ salt, so as to obtain a vanadium loading of 1 wt%. After the addition, the solution was stirred at room temperature for 2 h and at 70 °C for 5 h, and finally the mixture was dried by removing the excess solvent using a rotary evaporator. The calcination procedure of the materials was done as stated above for the synthesis of V-MCM-41.

Vanadium-immobilized catalysts were prepared as follows: To a stirred suspension of 1 g of Si-MCM-41 in toluene (60 ml), 2.2 mmol of 3-APTS was added slowly and then allowed to stirr overnight at 110 °C. The material was filtered, washed with toluene, soxhlet-extracted using a mixture of diethyl ether (100 ml) and dichloromethane (100 ml) for 24 h, and then dried under vacuum. The complexation of VO^{2+} ions on the organo-modified silica surface was done by stirring a suspension of 1 g of the organo-functionalized silica with a 0.01 M alcoholic solution of vanadyl sulfate for 5 h. The process was repeated twice for a maximum coordination of vanadyl groups on the functionalized silica surface and then it was filtered, washed with copious amounts of ethanol, and dried in an air oven at 80 °C for 3 h.

2.2. Characterization

Powder X-ray diffraction patterns of as-synthesized and calcined samples were recorded on a Rigaku D MAX III VC Ni-filtered Cu-Kα radiation, $\lambda = 1.5404$ Å, between 1.5 and 10° (2θ) with a scanning rate of 1°/min.

FTIR spectra of the solid samples were taken in the range of 4000 to 400 cm^{-1} on a Shimadzu FTIR 8201 instrument. Diffuse reflectance UV–vis spectra of the powdery samples were recorded in the range 200–800 nm in a Shimadzu UV-2101 PC spectrometer equipped with a diffuse reflectance attachment, using $BaSO_4$ as the reference. Specifically for the hydrated samples, the catalysts were kept under ambient conditions for 2 h while for the dehydrated samples, the catalysts were treated in dry air atmosphere at 550 °C for 5 h and flushed with an inert atmosphere, repeatedly, before the spectra were taken [17]. The samples were designated as hydrated (faintly yellowish) and dehydrated (white) samples, respectively. The absorption edge energy values were determined from the energy intercept of a linear fit passing through the near-edge region in a plot of $[F(R_\alpha) \cdot h\nu]^{1/2}$ vs $h\nu$, where the first parameter refers to the Kubelka–Munk (KM) function and $h\nu$ is energy of the incident photon.

The specific surface area, total pore volume, and average pore diameter were measured by the N_2 adsorption–desorption method using a NOVA 1200 (Quanta chrome) instrument. The samples were activated at 200 °C for 3 h under vacuum and then the adsorption–desorption was conducted by passing nitrogen over the sample, which was kept under liquid nitrogen. Pore-size distribution (PSD) was obtained by applying the BJH pore analysis applied to the desorption of nitrogen adsorption–desorption isotherms.

Temperature-programmed reduction was carried out on a Micromeritics Autochem 2910 catalyst characterization system, equipped with a TCD detector. The reduction was carried out in 5% H_2/Ar gas mixture flowing through the reactor at a rate of 20 ml/min and approximately 100 mg of the calcined sample was used for all the experiments. The temperature was then increased to 800 °C at a heating rate of 10 °C/min.

TG-DTA and DTG analysis of the catalysts were carried out on a Mettler Toledo 851 instrument using an alumina pan under air atmosphere (80 ml/min) from ambient to 1000 °C at a heating rate of 10 °C/min. The solid-state ^{13}C CP MAS NMR spectra were recorded on a Bruker MSL 300 NMR spectrometer with a resonance frequency of 75.5 MHz. The finely powdered samples were placed in 7.0-mm zirconia rotors and spun at 2.5–3.5 kHz, using glycine as the reference compound.

SEM micrographs of the vanadium-containing samples were obtained on JEOL-JSM-5200 scanning microscopy while the TEM images were performed on a JEOL JEM-1200 EX instrument with 100 kV acceleration voltages to probe the mesoporosity of the material.

2.3. Catalytic reaction

Oxidation reactions were performed in a stirred round-bottom flask fitted with a water-cooled condenser using 30 wt% aqueous H_2O_2 and 70 wt% aqueous TBHP as oxidants. The reactant mixtures of naphthalene (1 g, 7.8 mmol), H_2O_2 (30 wt%, 2.67 g, 23.56 mmol), and acetonitrile (10 g) solvent were added to catalyst (10 wt% with respect to naphthalene) and heated at a constant temperature of 80 °C under magnetic stirring (ca. 800 rpm) (Scheme 1). After reactions,

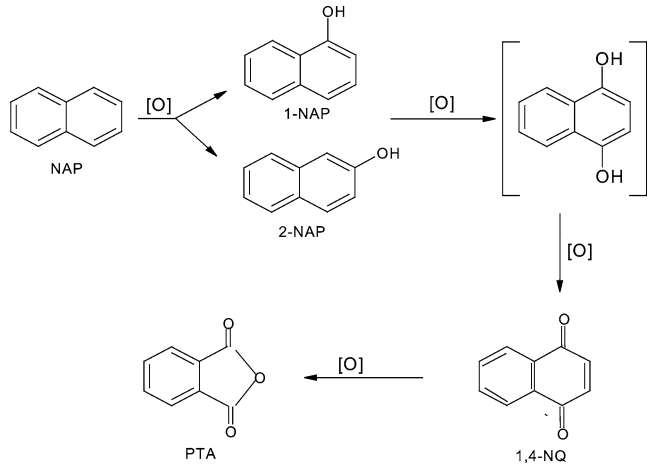

Scheme 1.

the reaction mixture was cooled to room conditions and the catalyst was separated from the reaction mixture by centrifugation and the oxidized products were analyzed on a gas chromatograph (HP 6890) equipped with a flame ionization detector (FID) and a capillary column (5 µm crosslinked methyl silicone gum, 0.2 mm × 50 m) and were further confirmed by GC-MS (Shimadzu 2000 A) and by injecting authentic samples. Leaching of the active metal sites during the reaction was verified mainly by the resubmission of the filtrate to the reaction conditions.

3. Results and discussion

3.1. Powder X-ray diffraction

XRD patterns of V-MCM-41, V–NH_2-MCM-41, and as-synthesized and calcined V/MCM-41 materials visualized in Fig. 1 show some important differences in the long-range ordering and characteristic diffraction patterns of mesoporous materials with the hexagonal structure. Even though it is known that a higher hydrothermal synthesis temperature can incorporate a greater percentage of metal on the silica framework, the sequential problem of the dissolution of micelles at higher temperatures limits our hydrothermal synthesis condition at 100 °C, as it largely affects the long-range ordering and peak intensities. The well-defined XRD patterns of the as synthesized Si-MCM-41 and V-MCM-41 samples can be indexed to the Bragg reflections *100*, *110*, *200*, and *210*, characteristic of materials with long-range ordering and their intensities are well pronounced. But after calcination a decreased intensity of the characteristic d_{100} peak with a corresponding disappearance of long-range ordered *210* peak is observed, showing a relatively well-ordered hexagonal structure of the materials. As observed by Reddy et al. [18], we also noted a slight shift of the characteristic (100) reflection to a lower angle with a corresponding linear increase in the *d* spacing and a_0 values with the percentage of vanadium loading for V-MCM-41 and the results obtained are listed in Table 1. The increase in the hexagonal unit cell parameter compared with its silica polymorph can be taken as an indication of the incorporation of vanadium, as the V–O bond distances are longer than the Si–O bond distances and the thickening of the pore wall due to transition metal promoted crosslinking of the amorphous silica walls [19]. But for V/MCM-41 and V–NH_2-MCM-41 samples, a decrease in intensity of the characteristic *100* peak and a gradual loss of long-range ordered peaks are noted (Fig. 1B), which shows the retainment of the mesopore structure with partial structural collapse and the results are more pronounced for the immobilized catalysts than the V/MCM-41 catalysts. These structural changes may arise from the inherent poor hydrothermal stability of M41S materials due to the high hydrophilicity derived from the presence of abundant surface silanols and thus high-temperature treatments can dissociate some of the pore walls and thereby affect its long-range ordering. Another interesting observation is the increase in unit cell parameter values of V/MCM-41 catalysts after calcinations, indicating that a part of vanadium atoms is incorporated on the framework positions of MCM-41. These kinds of results were obtained earlier for Nb/MCM-41 and this behavior is attributed not only to the extra framework species but also to the presence of lattice species [20]. Further no bands characteristic of the crystalline V_2O_5 phase is observed in any of the preparation methods ($2\theta > 20$) and hence it is assumed that the metal ions were either atomically dispersed in the framework positions of MCM-41 or may exist in an amorphous dispersed form on the outside surface of mesoporous support. Even though a proper comparison of the vanadium-incorporated and -grafted/immobilized cat-

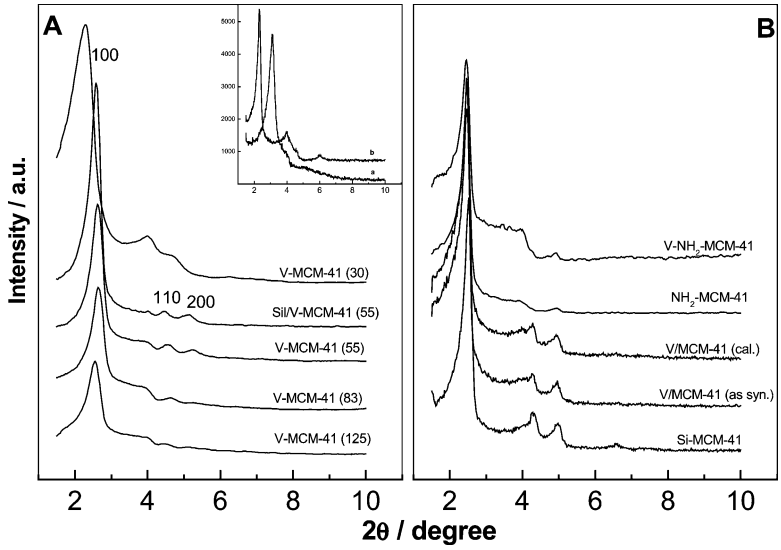

Fig. 1. X-ray diffraction patterns of (A) V-MCM-41 catalysts {inset, as-synthesized XRD patterns of (a) MCM-41 silica polymorph, (b) V-MCM-41 (55)}, (B) V/MCM-41 and V–NH_2-MCM-41 catalysts.

Table 1
Characteristics of vanadium-containing MCM-41 catalysts

Catalyst	V (mmol g^{-1})[a]	a_0[b] (Å)	S_{BET} (m^2 g^{-1})	V_p (cc g^{-1})[c]	Wall thickness[d] (Å)	TPR[e]	
						T_{max} (°C)	AOS
Si-MCM-41	0.0	40.49	845	0.6840	8.22	–	–
V/MCM-41 (C) [f]	0.196	41.48	797	0.6475	8.90	504	3.3
V–NH_2-MCM-41 (A)[f]	0.281	41.14	342	0.5813	11.51	Nd	Nd
V–NH_2-MCM-41 (C)	0.262	40.60	782	Nd	Nd	501	3.4
V-MCM-41 (55)	0.192	39.31	909	0.5376	15.72	412	4.5
V-MCM-41 (83)	0.135	38.62	828	0.4874	15.63	407	4.6
V-MCM-41 (125)	0.090	38.0	740	Nd	Nd	401	4.8
MCM-41 silica polymorph[g]	0.0	36.51	711	0.3707	14.52	–	–

Nd, not determined.
[a] Vanadium content determined by ICP-OES analysis.
[b] Unit cell parameter values calculated using $a_0 = 2d_{100}/\sqrt{3}$.
[c] V_p = pore volume.
[d] Wall thickness = $a_0 - D_p$, where D_p is the pore diameter.
[e] Temperature of maximum hydrogen consumption (T_{max}) and the average oxidation state (AOS) after reduction.
[f] Letters C and A in parentheses means calcined and as-synthesized samples while the numerals stands for Si/V molar ratios.
[g] Mesoporous support synthesized hydrothermally without the addition of vanadyl sulfate.

Table 2
IR band assignments and corresponding wavenumbers obtained for Si-MCM-41 and vanadium-containing MCM-41 catalysts

	ν (Si–OH)			
Catalyst	ν_{OH} (Si–OH)	ν_{as} (Si–O–Si)	{ν_{as} (Si–O–Si)/ν_{as} (Si–O–V)}	ν_s (Si–O–Si)
Si-MCM-41	3749	1080, 1230	972	801
V-MCM-41 (55)	3653	1078, 1224	976	805
V/MCM-41	3657	1078, 1228	974	804
V–NH_2-MCM-41	3710	1091, 1235	965	807

alyst is difficult, the well-ordered mesoporous patterns obtained for the vanadium-incorporated catalyst may be due to the simultaneous condensation between metal and silicon species in the presence of the organic micelles, thereby influencing largely the unit cell parameters, wall thickness, and the long-range ordering [21]. Thus it is reasonable to conclude that the observed differences after calcination may result from the loss of structural integrity after surfactant decompositions. However, for the grafted/immobilized catalyst systems, since the metal species are mainly on the surface the aforementioned interactions are limited and hence influence the peak broadening and the corresponding peak shifting to higher d spacing with the loss of long-range ordering. These results are better appreciated from Fig. 1A (inset) where the V-MCM-41 (55) material shows a highly intense XRD reflection with more ordered hexagonal structures than the parent silica polymorph prepared under the same conditions, but without any vanadium. Usually, the intensity of the *100* peak and the long-range ordered Bragg reflections are decreased and disappear with the amount and nature of metal incorporation. On the contrary, in the present case the structural ordering of the materials is increased up to an Si/V ratio of 55. However, when the Si/V ratio is 30, XRD patterns show the presence of a broad d_{100} reflection, with a decrease in the long-range ordered peaks and thus reveals that under hydrothermal synthesis conditions there exist an optimal molar ratio among the surfactant/silicate/heteroatoms and a possible change in any of them may cause drastic changes in its structural ordering. Hence, the more structural ordering of the Si/V = 55 catalyst explains the increased surfactant silicate interaction in the presence of metal salts as they compete to enter the silica framework and thus may act like a promoter for the extensive condensation of the silicate species and thereby for its reorganization.

3.2. FTIR spectroscopy

The presence of isolated surface silanols, hydrogen-bonded hydroxyl groups, and amorphous structures of the wall are evidenced from the IR spectrum of the calcined Si-MCM-41 samples. The band at 1080 cm^{-1} is assigned to the asymmetric ν_{as} (Si–O–Si) vibrations and the band at 800 cm^{-1} is assigned to symmetric vibrations of Si-MCM-41, while the band at 970 cm^{-1} is attributed to ν (Si–OH) vibrations (Table 2, Fig. 2) [22]. In the hydroxyl region (3600–3200 cm^{-1}) a broad band is seen, assigned to the silanol groups inside the channels of Si-MCM-41 and the decreased intensity of the silanol groups after vanadium grafting shows the active participation of the surface silanols in bond formation with the vanadia precursor, $VO(acac)_2$. Indeed, it is reported that the vanadyl complex gets anchored on the hydroxyl groups of the support either by hydrogen-bonding interactions between the pseudo-π system of the acac ligand and the silanols or by a ligand exchange mech-

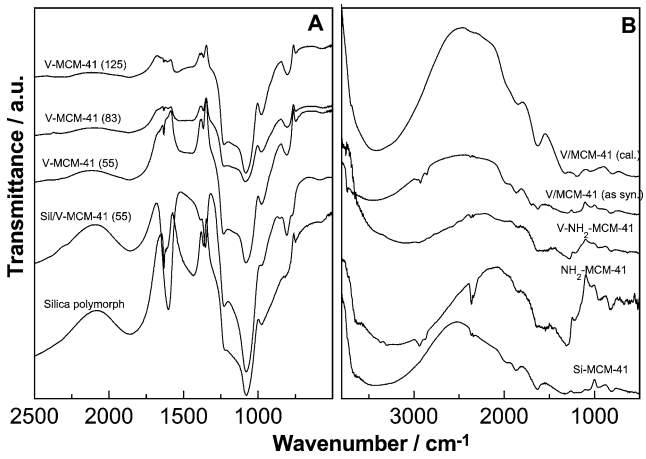

Fig. 2. Infrared spectra of (A) V-MCM-41 catalysts, (B) V/MCM-41 and V–NH_2-MCM-41 catalysts.

anism [23]. Further, the grafting of $VO(acac)_2$ is confirmed by the presence of bands in the region of 1600–1200 cm^{-1} and at 2950–2850 cm^{-1}, since these vibrations are attributed to the presence of acetyl acetonate ligands of the adsorbed complex [24]. After calcination at 500 °C, all the bands belonging to the organic groups disappeared which proves the removal of acetyl acetonate and the formation of VO_x inside the pores of the mesoporous support. For the immobilized NH_2-MCM-41 material weak bands at 2940 cm^{-1} and at 1540 cm^{-1} are observed which are assigned to the C–H stretching and N–H bending vibrations, respectively [25]. A thorough examination of the amine peaks after metal immobilization shows that the peak values are shifted to lower wavenumbers and the decrease in wavenumber indicates the possible anchoring of the metal species on the active sites. These results further prove that the organosiloxane groups had linked to the silica surfaces by condensation reactions, for the formation of Si–O–Si bonds, and not through electrostatic interactions or by hydrogen-bonding interactions between the amine groups and the Si–OH groups. The successful immobilization of the propyl amino groups on MCM-41 was further confirmed from the C:N values obtained from the elemental analysis study and ^{13}C CP MAS NMR spectra. For the V-MCM-41 catalysts intense bands are visible in the range 980–950 cm^{-1}, and an increased intensity with a corresponding peak shifting to higher frequency is noted with the increase in the percentage of vanadia loading. Since Si-MCM-41 also shows peaks in this region, due to the rocking mode vibrations of the Si–OH groups, in the literature its assignment is described with uncertainty. However, the shifting of 960 and 1090 cm^{-1} peaks to lower and higher frequencies, respectively, and their sharpness can be taken as an indication of the incorporation of metal species in the framework of the mesoporous materials [26]. Indeed silylated V-MCM-41 catalysts show a progressive increased intensity for the 960 cm^{-1} band and hence can be reasonably concluded that the band position at 960 cm^{-1} is attributed to Si–O–V band positions, as these kinds of assignments are noted earlier for titanium-containing mesoporous materials [14]. Moreover, no peaks are observed at 1020 and at 820 cm^{-1} characteristic of V=O stretching vibrations and V–O–V deformation modes of crystalline V_2O_5 [27], as already observed from the XRD measurements. So from the above results, it is interpreted that the formation of vanadyl polymers is limited or it may be in a highly dispersed state on the high surface area support and thus its presence is not so prominent.

3.3. BET measurements

The surface area of the catalysts determined by the BET method shows that with the percentage of vanadia loading the surface area is increased for V-MCM-41 samples while for V/MCM-41 and V–NH_2-MCM-41 catalysts the surface area is decreased, due to the presence of the bulkier organic moieties inside the pore channels. For the V–NH_2-MCM-41 catalysts, the silylation of 3-APTS may tend the organo amino groups to occupy defect sites in the pore walls as self-assembled monolayers and thus reduce the adsorption sites for the nitrogen molecules, contributing to a decreased surface area. Interestingly, after calcination, the surface area of the impregnated and immobilized materials had shown an increase from their grafted/anchored counterparts, and may be due to the removal of the bulky acetyl acetonate/organo amino groups and the BET results obtained are summarized in Table 1. The support silica polymorph shows a surface area of 711 m^2/g and an increase of 198 m^2/g is observed for the V-MCM-41 (55) catalyst. However, the grafted V/MCM-41 and the immobilized V–NH_2-MCM-41 material show approximately 28 and 59% surface area decrease than Si-MCM-41, which is restored to almost 90% of the original value after calcinations. N_2 adsorption–desorption isotherms of the silica polymorph, V-MCM-41 (55), V/MCM-41, NH_2-MCM-41, and V–NH_2-MCM-41 materials show an inflection in the P/P_0 range of 0.2–0.35, with completely reversible isotherms but with little hysteresis, characteristic of ordered mesoporous materials of Type IV according to the IUPAC classification (Fig. 3A). The hysteresis loop observed in the high-pressure region for the MCM-41 sample may result from the agglomerization of particles of the mesoporous materials. Moreover, as the hydrothermal treatment is prolonged the step in the capillary condensation in the mesopore is sharper and shifts to higher pressure regions, influenced by narrowness in the pore-size distribution curve with a corresponding pore-size enlargement [28]. These results are further illustrated from the BJH pore-size distribution as all samples show sharp peaks in the range 20–30 Å attributed further to the mesopore ordering with well-defined pore structures (Fig. 3B). Usually for M41S-related materials during metal incorporation, the metal species may interact with the surface hydroxyl groups and may contract the pore walls resulting in a decreased pore size. However, in the present case an increase in pore size is noted with the percentage of metal incorporation, which fur-

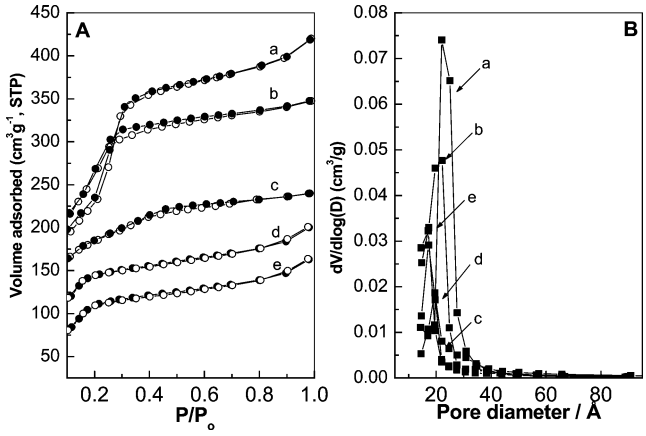

Fig. 3. Nitrogen adsorption–desorption isotherms (A) and pore-size distribution profiles (B) of (a) V/MCM-41, (b) V-MCM-41 (55), (c) silica polymorph, (d) NH_2-MCM-41, (e) V–NH_2-MCM-41.

ther suggests that vanadium is incorporated deep inside the silica framework, as observed for zeolites, and is in accordance with the earlier XRD results [29]. These results can be further confirmed by the ease of metal reduction during reduction measurements and are discussed in a later section.

3.4. UV–vis spectroscopy

Diffuse reflectance UV–Vis spectra is a useful technique for gaining information about the coordination environment and oxidation states of vanadium species in various molecular sieves/oxide surfaces. The UV–vis spectra of V-MCM-41 (cal.), V/MCM-41 (as syn., cal.), and V–NH_2-MCM-41 (as syn.) samples are given in Fig. 4 and the deconvoluted peak assignment proportions are given in Table 3. The band at 220 nm is typical for siliceous materials but new bands appeared in the 250–500 nm range after vanadium incorporation and their intensity is increased with the percentage of vanadia loading. Indeed, direct information about the oxidation state and dispersion of vanadia species can be interpreted from the color of the materials prepared. The as-synthesized V-MCM-41 catalysts are white while the V/MCM-41 and V–NH_2-MCM-41 are pale green in color and on the basis of the appearance of green color, weak absorptions in the longer wavelength can be interpreted [14]. Even though the species anchored on the amino groups are V^{4+}, drying of the catalyst at 80 °C may change its oxidation state from +4 to +5, and hence the intensities of the UV–vis peaks in the 600–800 nm regions are not so prominent and/or the decreased intensity in the low-frequency region arises, as the d–d transitions are generally 10–30 times lower than the highly intense charge transfer (CT) transitions in the range of 260–360 nm [6]. Further, the color of the dehydrated calcined catalysts (V-MCM-41, V/MCM-41) is white and on hydration (contact with atmosphere) the color changes to yellowish for the V/MCM-41 catalysts. However, for V-MCM-41 catalysts its a very slow process which may be due to the modification in the oxidation state of the vanadia species (V^{5+}) from the isolated tetrahedral coordination (T_d, 260 nm) to its square pyramidal/distorted octahedral coordination (O_h, 350–450 nm) by contacting with two water molecules in the atmosphere due to the high hydrophilic nature of the catalyst and the red shift is increased with the percentage of vanadia loading. The possible and abrupt color transformation of calcined V/MCM-41 catalysts further indicates that a higher percentage of vanadium atoms are on the wall channels of V/MCM-41, hence the water molecules can easily access the site for higher coordination. Furthermore, after calcination the vanadium species located on the

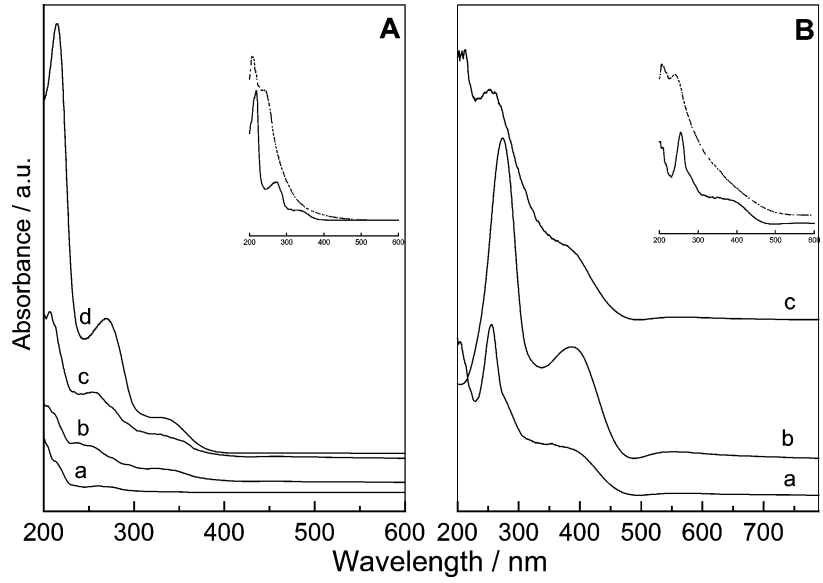

Fig. 4. Diffuse reflectance UV–vis spectra of (A) (a) silica polymorph, (b) V-MCM-41 (125), (c) V-MCM-41 (83), (d) V-MCM-41 (55), (B) (a) V/MCM-41 (as syn.), (b) V/MCM-41 (cal.), (c) V–NH_2-MCM-41 (as syn.), recorded under ambient conditions, inset in (A) shows the hydrated (solid line) and dehydrated (dotted line) spectra of V-MCM-41 catalyst while (B) shows the hydrated and dehydrated spectra of V/MCM-41 catalyst.

Table 3
Relative proportion of component peaks in UV–vis spectra of vanadium-containing mesoporous materials and their corresponding absorption edge energy values

Catalyst	240–270 nm	320–340 nm	> 360 nm	Absorption edge energy value (eV)	Local symmetry
V–NH_2-MCM-41 (A)	67.58	12.19	20.21	2.70	–
V–NH_2-MCM-41 (C)	72.97	6.32	20.70	2.60	–
V/MCM-41 (C)-H[a]	64.68	6.81	28.51	2.57	–
V/MCM-41 (C)-D[a]	72.83	27.16	0.0	3.25	
V-MCM-41 (55)-H	74.95	25.05	0.0	3.31	–
V-MCM-41 (55)-D	90.10	9.90	0.0	3.60	–
V_2O_5	–	–	–	2.30	Square pyramidal
NH_4VO_3	–	–	–	3.23	Distorted tetrahedral
Na_3VO_4[b]	–	–	–	3.21	Tetrahedral

[a] H, hydrated; D, dehydrated.
[b] From Ref. [33].

surface enhances the formation of M–O–M bonds predominantly than Si–O–M bonds and these may also enhance the formation of polymeric V–O–V-like species, thus accounting for the formation of bands after 360 nm, which are not evidenced from the XRD and IR measurements. Thus the observed increase in the intensity of the bands above 330 nm can be equally due to the larger polymerization of the surface vanadium sites and/or to the change in the nature of the tetrahedral vanadium sites to higher coordinated metal sites. However, it is interesting to note that the dehydrated catalysts show a greater percentage of tetrahedral vanadium species in the peak fitting curves and are almost devoid from the band above 330 nm. In detail, the dehydrated V-MCM-41 (55) catalyst shows ∼ 90% of T_d species, in the 240–280 nm region, while the dehydrated V/MCM-41 catalyst shows an almost disappearance of the 360 nm peak, which further shows the high affinity of atmospheric water molecules to form coordination with the surface T_d vanadium species to penta- or hexacoordinated vanadium sites (Fig. 4, inset). In order to extract the exact nature of different vanadia species and to investigate its local environment on the MCM-41 surface, absorption edge energy measurements were also performed by a procedure reported by Barton et al. [30], with reference to vanadium model compounds of known local symmetries. Usually the edge energy values of the V^{4+} are in the 4.5–5 eV energy region while the O^{2-} to V^{5+} ligand to metal charge transfer are in the 2–4 eV edge energy region [31]. From Table 3 and comparison with vanadium model compounds, it is apparent that all the edge energy values are in the range 2.5–3.5 eV and hence it is reasonable to assume that the formation of tetrahedral-like V^{5+} species are more for V-MCM-41 catalyst systems, while the postsynthesis modified catalysts are more vulnerable toward higher coordinated octahedral like species. However, careful examinations shows that V-MCM-41 catalysts produce a higher edge energy value than the grafted and immobilized calcined catalyst systems and thus points toward a decrease in vanadium domain size or a change in coordination of the vanadium cations [32]. Thus vanadium ions in V-MCM-41 samples can be tentatively attributed to be tetrahedrally coordinated, supporting the framework incorporation. Further, literature shows that the difference in edge energy values depends on the support material and to the surface density of VO_x species and in the present case as the support is the same for all the catalyst systems the observed difference in the $h\nu$ values may arise unambiguously from different surface vanadium species.

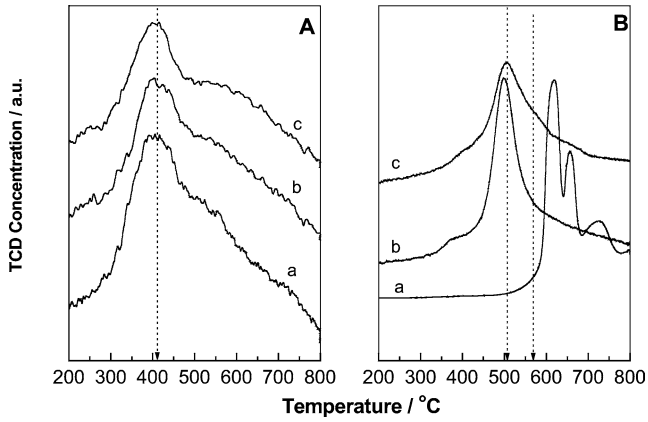

Fig. 5. H_2-TPR reduction profiles of (A) (a) V-MCM-41 (125), (b) V-MCM-41 (83), (c) V-MCM-41, (55), (B) (a) pure V_2O_5, (b) V–NH_2-MCM-41 (cal.), (c) V/MCM-41 (cal.).

3.5. *Temperature-programmed reduction*

H_2-TPR profiles of the catalysts taken in the 100–800 °C temperature range show that the reduction temperature maxima (T_{max}) and the average oxidation state (AOS) values vary considerably in the incorporated and grafted/immobilized catalyst systems as given in Table 1 and visualized in Fig. 5. V-MCM-41 catalysts exhibit sharp reduction peaks in the range 400–420 °C and the peak maxima is shifted to higher temperature regions as the loading is increased and may result from the reduction of monomeric or low oligomeric surface-dispersed tetrahedral vanadia species. In contrast to the V-MCM-41 catalyst systems, V/MCM-41 materials show a very sharp peak at 510 °C, and a distinct tail at ∼ 570 °C, indicating the formation of

less reducible "bulk-like" vanadia species, which may exist in a highly dispersed state on the support surface [33,34]. The TPR profiles of the immobilized catalysts (after calcination at 540 °C) also show peak maxima at 505 °C, but interestingly the profiles are devoid of the shoulder-like peaks (∼ 570 °C), as observed with the grafted catalysts. Thus it can be noted that immobilization provides a probable $(–(CH_2)_3–NH_2)_3VO^{2+}$ anchoring of amino groups and the vanadyl ions and hence during calcination these organic spacers largely inhibit the agglomerization of the vanadia species and hence the formation of bulk-like vanadia species is not prominent. Even though the observed reduction temperature maxima of the V-MCM-41 catalyst is lower than the literature reports, such ease of metal reduction is observed earlier for framework-incorporated V-MCM-41 samples by Grubert et al. [35]. Moreover, it is pointed out that in addition to the material characteristics, the reduction temperature and the average oxidation state values also depend on the reduction conditions like H_2 partial pressure, heating rate, and final reduction temperature and hence comparison of the reduction values is inappropriate as they show variations with the experimental setup procedures [36]. In short, it can be concluded that the vanadia species incorporated in V-MCM-41 catalysts are reduced at lower temperatures than the vanadium species in grafted catalyst and thus suggests the presence of trace amounts of bulk-like particles in the V/MCM-41 catalyst, which shifts the TPR peaks to higher temperatures. In other words, when incorporation of metal species in silica walls is possible, the formation of M–O–M linkages will be less favorable and better dispersion of metal sites are obtained than grafting/impregnation methods of similar metal loadings [21]. However, all the TPR profiles were entirely different from pure V_2O_5 and hence conclude that V_2O_5 formation is not so predominant in any of the preparation procedures since bulk V_2O_5 is reduced only at temperatures above 600 °C (Fig. 5B (a)). Further it can be observed from Table 1 that the average oxidation state value of vanadium in the reduced catalysts is larger in the postsynthesis modified catalysts than in the hydrothermally synthesized catalysts. These results further conclude the formation of small amounts of V_2O_5 microcrystallites on the V/MCM-41 catalysts, which are reduced to a greater extent than the isolated vanadium sites in V-MCM-41 [37].

3.6. Thermal analysis

The thermal analysis curves of Si-MCM-41, V-MCM-41, and V-NH_2-MCM-41 materials are depicted in Fig. 6. The DTG-DTA spectra of the as-synthesized Si-MCM-41 and V-MCM-41 show that the entire template, including the water adsorbed on the hydroxyl groups of the pores, is lost at a temperature of ∼ 400 °C when heated under air flow. In detail, the TGA patterns of Si-MCM-41 show a sharp weight loss below 100 °C corresponding to the loss of physisorbed water and further weight loss extends in the regions of 150–300 and 300–380 °C, attributed to the decomposition of the template (CTMABr) occluded in the pores [38].

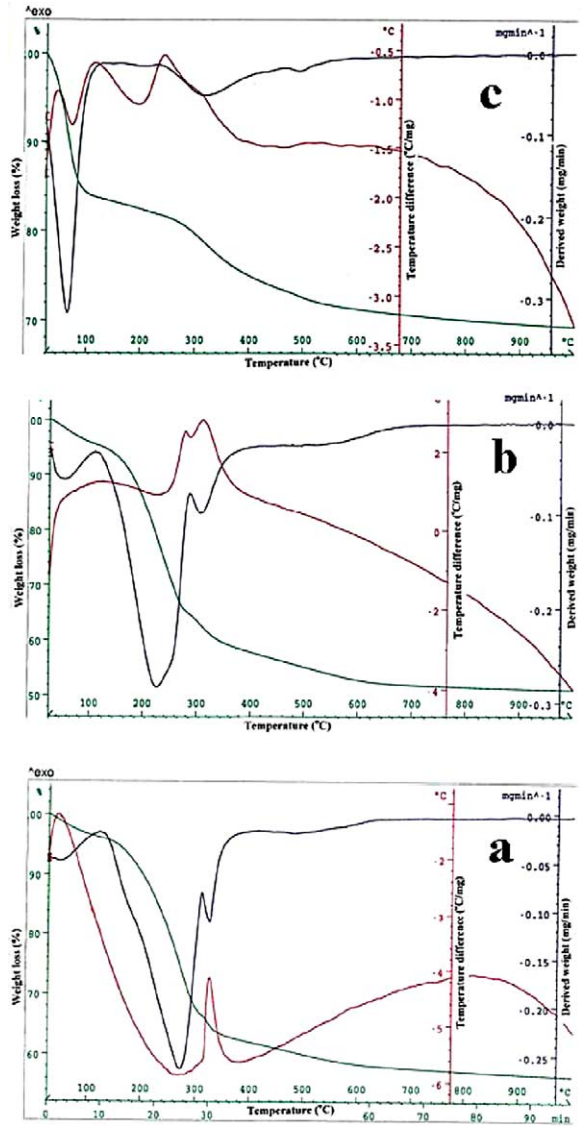

Fig. 6. TGA-DTA curves of (a) Si-MCM-41, (b) V-MCM-41 (55), (c) V–NH_2-MCM-41.

The TG/DTG spectrum of the V-MCM-41 (55) catalyst also shows an almost similar thermal pattern as that of Si-MCM-41 material. The sharp weight loss observed below 100 °C corresponds to the loss of physisorbed water molecules while a further decomposition pattern extends to 200–250 and 300–350 °C, attributed to the combustion of hexagonally packed surfactants. However, a detailed examination shows that the percentage weight loss of the surfactants is larger for V-MCM-41 catalysts (> 43%) than the corresponding silica polymorph (> 35%, figure not shown). These results are better appreciated in comparison with the XRD patterns of V-MCM-41 and its corresponding silica polymorph, where the V-MCM-41 (55) shows a better long-range ordered and more intense XRD pattern than the parent Si-MCM-41. These results further support our above inter-

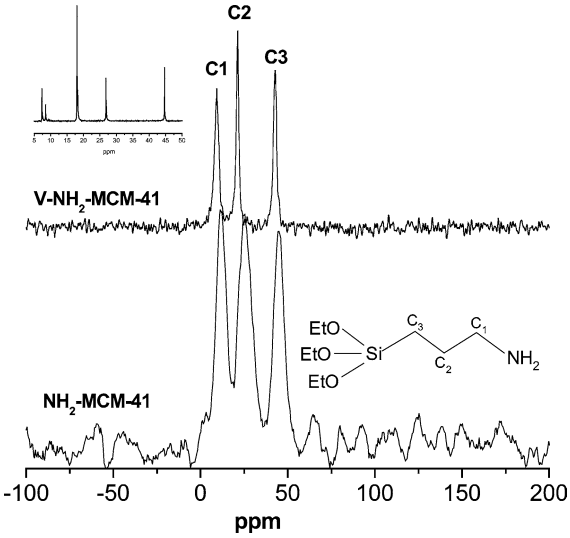

Fig. 7. ^{13}C CP MAS NMR spectra of (a) NH_2-MCM-41, (b) V–NH_2-MCM-41 and 3-APTS (inset).

pretations and thus can be concluded that the interaction between the surfactant/silicate is greater in presence of the metal salts, at least in the present hydrothermal synthesis, and hence induces a better arrangement of the hexagonal structure and/or the bigger pore size of V-MCM-41 may be responsible for the higher amount of weight loss.

On the contrary, the TG/DTG patterns of the NH_2-MCM-41 (figure not shown) and V–NH_2-MCM-41 catalysts (Fig. 6c) show a weight loss below 100 °C and a sharp, distinct weight loss at 300–350 °C and at 500–600 °C. As noted the former weight loss arises from the desorption of physisorbed water while the second peak develops from the burning of the amino propyl groups from the pores of the support surface and the third peak arises due to the water loss formed by the condensation of the silanol groups [39,40]. The DTA pattern further supports the above results as it shows a strong exothermic peak around 320 °C, and thus these loss are attributed to the decomposition of the grafted 3-APTS groups.

3.7. ^{13}C CP MAS NMR spectroscopy

The presence of 3-APTS group and its chemical nature on the support surface are further exploited by the NMR techniques. The solid-state ^{13}C CP MAS NMR spectra of NH_2-MCM-41 and V–NH_2-MCM-41 and the liquid-state NMR spectra of 3-APTS (for comparison, inset) are given in Fig. 7. The peak observed at 11.3 ppm can be accounted for the carbon atom (C^1) adjacent to the amino groups while the peaks at 25.9 and at 45.1 ppm belong to the central carbon atom (C^2) and the carbon atom adjacent to the silicon moiety (C^3) of the 3-APTS, respectively [4]. A careful examination of these peaks shows that after immobilization of VO^{2+} ions, the peak positions are changed to lower ppm values of 9.3 (C^1), 21.5 (C^2), and 43.3 (C^3), respectively.

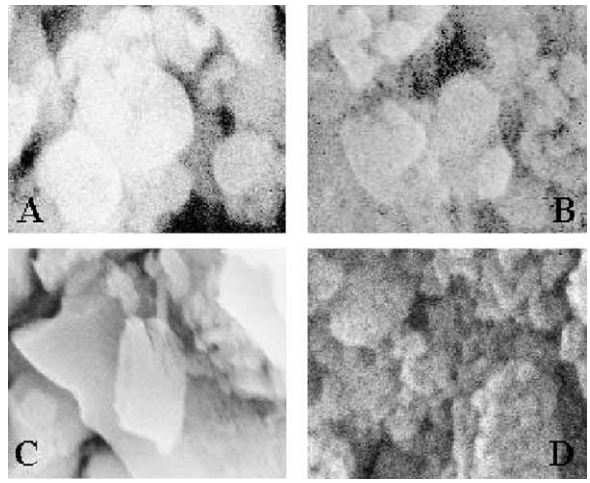

Fig. 8. Scanning electron micrographs of (a) silica polymorph, (b) V-MCM-41 (55), (c) V/MCM-41, (d) V–NH_2-MCM-41.

3.8. Electron microscopy

The particle size and morphology of Si-MCM-41, V-MCM-41, V/MCM-41, and V–NH_2-MCM-41 samples were determined by SEM analysis and are shown in Fig. 8. The micrographs show some important differences in the morphology of the catalysts after metal incorporation and post-synthesis modifications where the hydrothermally synthesized V-MCM-41 (55) catalyst shows a distorted hexagonal structure (ca. 1.1 μm in diameter). However for the V/MCM-41 catalysts, large flake-like structures (ca. 1.4 μm) are observed while the immobilized catalyst shows an apparent decreased grain size (ca. 0.3 μm) with large disorder from the hexagonal structure and thus illustrates that various treatment conditions can affect/modify the morphological structure (shape, size) of the MCM-41 surface considerably. TEM analysis of V-MCM-41 (55) catalyst shows the presence of hexagonally arranged pore structures, when viewed along the pore direction, and the presence of parallel lattice fringes, on a side view analysis (Fig. 9a and 9b). The presence of equidistant parallel fringes shows the nature of separation between the layers and the well-packed unique arrangement further points to the addition of such monolayers [38]. These kinds of results are valuable as they supports the assumption that the deposition of 2–3 monolayers of silicate precursor on the isolated surfactant micellar rod with its subsequent further condensation results in the formation of long-range ordered mesoporous materials [5]. Furthermore, a comparison of the TEM images (Fig. 9c and 9d) shows that the materials prepared by postsynthesis methods had essentially damaged the regular structural ordering of the mesoporous materials and are more pronounced for the grafted calcined sample.

3.9. Catalytic oxidation of naphthalene

The reaction rates obtained for V-MCM-41, V/MCM-41, and V–NH_2-MCM-41 catalysts in the oxidation of naphtha-

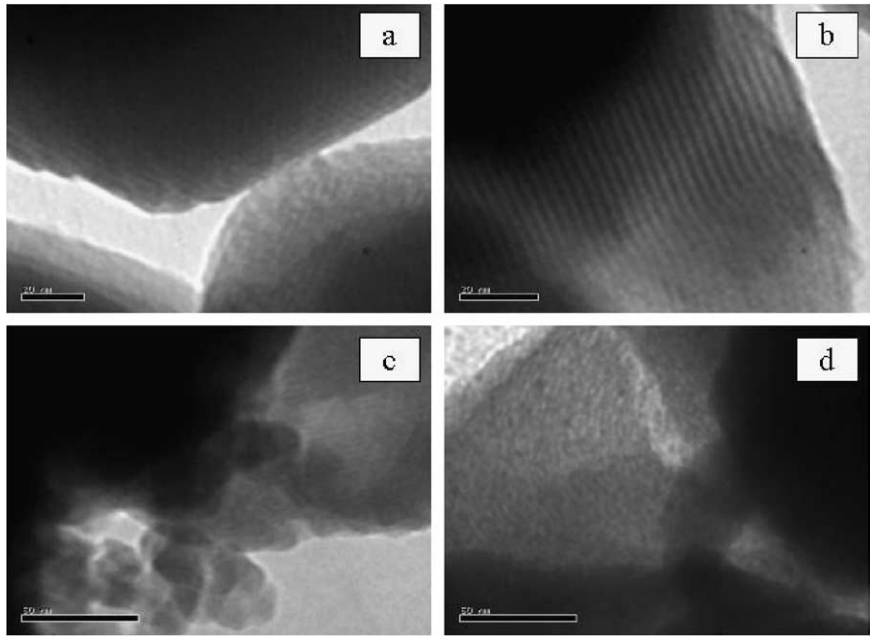

Fig. 9. TEM images of (a) V-MCM-41 (55) (viewed along the pore direction), (b) V-MCM-41 (55) (parallel fringes, side on view), (c) V–NH_2-MCM-41, (d) V/MCM-41.

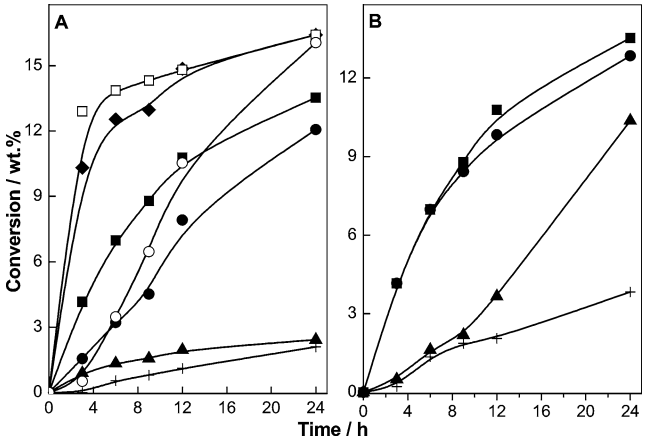

Fig. 10. (A) Influence of reaction time on the conversion and selectivity of naphthalene oxidation over (■) V-MCM-41 (55), (●) V-MCM-41 (83), (▲) V-MCM-41 (125), (+) Sil/V-MCM-41 (55), (◆) V/MCM-41 (as syn.), (□) V/MCM-41 (cal.), (○) V–NH2-MCM-41. (B) Various leaching studies performed on V-MCM-41 (55) catalysts: (■) fresh cycle, (●) resubmission of the catalyst removed filtrate after 3 h of run, (▲) application of stirred solvent/oxidant filtrate mixture to the reaction conditions with substrate, (+) submission of the catalyst to the reaction conditions after stirring in an ∼ 1 M H_2O_2 solution.

lene are visualized in Fig. 10A. Interestingly, it is possible to gain a better insight into the catalytic properties from a comparison of the conversion profiles of the three different catalyst systems. For V-MCM-41 and V–NH_2-MCM-41 catalysts, the conversion increases gradually with time and reaches a maximum of 13.5 and 16.0%, respectively, after 24 h of the run. However, for the V/MCM-41 catalyst the conversions are abrupt at the early stages of the reaction and are almost steady throughout the run and show 16.4% naphthalene conversion after 24 h. The slightly lower catalytic activity of the V-MCM-41 material shows that the vanadium sites are not completely accessible for the diffused reactant molecules due to the partial structural collapse of the mesoporous material under such drastic reaction conditions. Screening of the catalysts in a wide temperature range of 60–80 °C shows that higher temperature helps to attain a maximum conversion rate with respect to substrate and the choice of oxidant follows that TBHP (70%) gives negligible reaction rates, while shifting the oxidant from TBHP to dilute H_2O_2 (30%) increases the conversion rates drastically. Further, it is known that solvents had a profound influence on the catalytic activity and selectivity in liquid-phase oxidation reactions as they can tremendously influence the mass transport and diffusional problems, especially with porous solid supports. Moreover, using molecular sieves as catalyst, the choice of solvents is crucial as the molecular sieve itself can act as a second solvent, which extracts the substrate molecules form the bulk solvent and this interaction may largely affect on what solvent had been used for the reaction. Hence in the present reaction of naphthalene oxidation, the activity of the catalysts was thoroughly verified in a series of solvents with different polarities. The reaction rates observed under various solvents, as shown in Fig. 11, follow the order $CH_3CN > (CH_3)_2CO > C_2H_5OH$. The enhanced activity of the V-MCM-41 (55) catalyst in acetonitrile than ethanol can be explained twofold:

(a) with acetonitrile, an aprotic solvent, the phase separation between the aromatic substrate part and the aqueous oxidant part is greatly decreased and thereby allows the

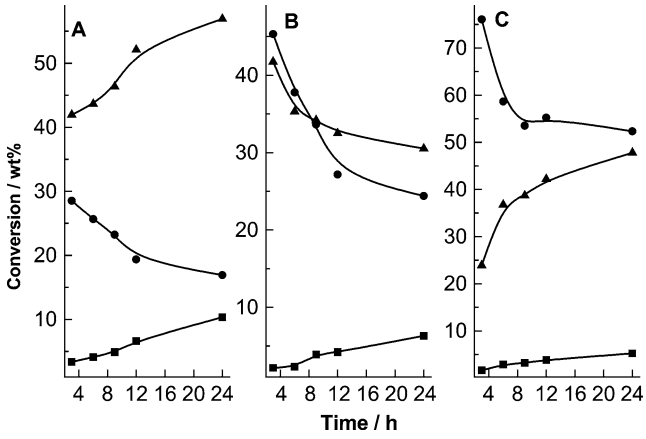

Fig. 11. Influence of solvents on the conversion and selectivity of naphthalene oxidation over V-MCM-41 (55) catalyst, (A) CH_3CN, (B) $(CH_3)_2CO$, (C) C_2H_5–OH, where (■) stands for conversion rates while (▲) and (●) stand for pthallic anhydride and quinone selectivity.

easy transport of the active oxygen species for the oxidation process [41], and

(b) it is known that the activity of the catalysts is increased with the solvent polarity and hence acetonitrile having more polarity helps to attain the vanadium peroxo species preferentially.

Indeed the higher the solvent polarity, the higher the concentration of the substrate on the active metal sites and thus the increased reaction rate.

Furthermore, in the oxidation of naphthalene as shown in Scheme 1, the polarity of the reactant (naphthalene) and the primary products formed (napthols) are different: the reactant is nonpolar while the primary products are polar. Hence hydrophobic catalysts can enhance the conversion rates as it can suitably adsorb the reactant molecules while hydrophilic catalysts can adsorb the formed napthols preferentially and thereby convert them to their further oxidized products. In line with the above assumptions, an interesting observation is the difference in the selectivity behavior of the V/MCM-41 catalysts before and after calcinations, as the grafted catalyst shows the formation of hydroxylated products during the initial stages of the reaction (> 15%/6 h) while its calcined counterpart shows only the presence of more oxidized products without any hydroxylated primary products. So it is assumed that hydrophilic–hydrophobic interactions also play a deciding role in the selectivity of hydroxylated products during hydroxylation reactions. Since the presence of bulkier organic groups on the as-synthesized V/MCM-41 catalyst makes the catalyst surface genuinely hydrophobic, the oxidation of naphthalene will be more than that of napthols, as these compounds desorbed rapidly from the hydrophobic surface of the as-synthesized V/MCM-41 material. However for the calcined V/MCM-41 catalyst, since calcination decomposes all the organic moieties the surface becomes more hydrophilic and thus the oxidation of napthols is more pronounced. These kinds of results are noted earlier for titanocene dichloride (Cp_2TiCl_2)-grafted MCM-41 catalyst in the liquid-phase hydroxylation of benzene, where the activity of the grafted catalysts is close to 80% with a phenol selectivity of 90% [42]. But after calcination the selectivity decreased drastically to 50%, and the authors highlight this difference to the retrieval of the hydrophilic nature after the removal of the bulkier Cp ligands and thus to the selectivity difference. Even though the mode of interaction and coordination sites of $VO(acac)_2$ and Cp_2TiCl_2 are different, the observed differences in the selectivity behavior unambiguously derives from the hydrophilic–hydrophobic interactions but the activity difference of the two catalyst may lie in the redox nature of the two 3d transition metals (Ti, V), since it is known that the lower the outer *d* electron density, the stronger the capacity to enhance the activation of H_2O_2 and thus shows the difference.

3.10. Investigation of catalyst stability

Heterogeneity/stability of the catalysts was investigated in detail using a series of leaching studies and regeneration measurements, giving much attention to the V-MCM-41 catalyst systems. Literature reveals that vanadium-containing mesoporous catalysts show leaching of active metal components during liquid-phase oxidation reactions and hence in order to obtain more insight we opted for such a drastic reaction condition. Application of the used catalysts by simple washing with $CHCl_3$ and washing followed by calcination showed a decrease in activity of the V-MCM-41 and V/MCM-41 catalyst systems. Indeed in both cases, no pthallic anhydride (PTA) was detected and hence infer the loss of weakly bonded extraframework vanadia species, thereby decreasing the further oxidation of quinone products. However, according to Sheldon et al. [43], the heterogeneity of a catalyst can be better addressed only if the catalyst applied under reaction conditions will be removed in half of the run and by the resubmission of the filtrate under similar reaction conditions. Accordingly, resubmission of the filtrate under the reaction conditions (for V-MCM-41 and V/MCM-41) shows an enhancement in conversion rate, pointing out that some of the vanadium atoms on the wall surface are leached out during the run and thus the observed enhanced activity of the fresh catalysts may result from the leached vanadia species, shown in Fig. 12. In order to attain more evidence for what causes the exact leaching phenomenon in this reaction, two separate leaching studies are also performed with the V-MCM-41 (55) catalyst. The catalyst was first stirred in an acetonitrile/oxidant mixture for 2 h at 80 °C and the filtrate is applied under the reaction conditions with the addition of substrate. A second experiment was performed by stirring the catalyst in the presence of H_2O_2 (∼ 1 M) for 2 h and the procedure is repeated as above, with the treated catalyst and substrate under the reaction conditions, depicted in Fig. 10B. Interestingly, for the reaction, the "catalyst" stirred in H_2O_2 solution and applied to the reaction conditions shows a decreased conversion rate

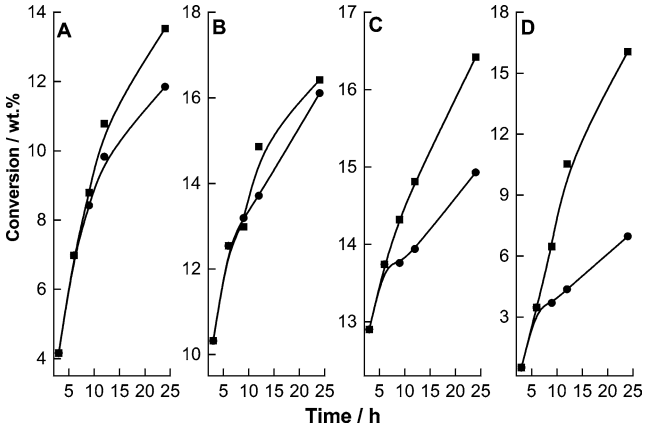

Fig. 12. Hot filtration experiments of different vanadium-containing MCM-41 samples: (A) V-MCM-41, (55) (B) V/MCM-41 (as syn.), (C) V/MCM-41 (cal.), (D) V–NH_2-MCM-41 where (■) stands for fresh and (●) for filtration after 3 h of the run.

while the "filtrate" obtained from the solvent/oxidant mixture shows an increased conversion rate; this concludes the major role of oxidants in the leaching of active metal sites. Hence in order to compare the stability of vanadium species in and on the MCM-41 framework, the V/MCM-41 catalyst was also stirred in an ~ 1 M aqueous H_2O_2 solution. Interestingly, the treated V/MCM-41 catalyst shows almost null activity even after 24 h and hence concludes that the vanadium atoms introduced into the crystalline framework are more stable than those grafted on the mesoporous support surface. However, for the V–NH_2-MCM-41 catalyst, the high-density amino groups on the mesoporous support surface tend to bind the VO^{2+} ions effectively, thus pointing to the increased heterogenity of the immobilized catalyst (Fig. 12d) than the other two vanadium-containing catalysts. Thus the stability of vanadium-containing catalysts prepared by different methods, under the present reaction condition, can be rationalized in the following order, V–NH_2-MCM-41 > V-MCM-41 > V/MCM-41.

The decreased heterogenity of the calcined V-MCM-41 catalyst can be explained in detail: since V-MCM-41 is a hydrophilic catalyst, due to the presence of abundant surface silanols, the interaction of aqueous H_2O_2 (30 wt%) will be more on the defect sites of the mesoporous material and thus can detach some of the vanadia species residing on extra framework positions (species observed in the UV–vis spectra, > 320 nm). This assumption is supported by the point that TBHP (70 wt%) had shown a decreased conversion rate under the present reaction conditions as the bulkier hydrophobic organic groups interaction will be limited on the hydrophilic catalyst surface compared with the dilute H_2O_2 oxidant and/or to the lesser percentage of active oxygen content than H_2O_2 (for H_2O_2 the active oxygen content is 47% while for TBHP it is 7.5%). Hence, in order to further address these matters we have done silylation on V-MCM-41 (55) catalysts with dichlorodimethylsilane and interestingly under identical reaction conditions, they show a drastic decrease in activity than the V-MCM-41. Since the silylation procedures effectively consume the silanol groups, a drastic change in the physical properties of the material from hydrophilic to hydrophobic is developed and thus the interaction of oxidant/substrate on the defect sites may decrease. Furthermore, the decreased heterogenity of the V-MCM-41 catalysts may essentially arise from (i) calcination treatment itself, as during calcination the water formed due to the decomposition of the template molecules can break some of the Si–O–V bonds and these species get leached out and dispersed on the support surface, similar to impregnated metal complexes, which can easily change its coordination state even with the atmospheric moisture, (ii) usage of aqueous H_2O_2 as oxidant makes the vanadium T_d sites to form the catalytically active vanadium peroxo complex species, which are not stable in the reaction medium, and hence changes its coordination from T_d to O_h by contacting with water molecules. (iii) Moreover, under drastic oxidation reaction conditions even the mesopore wall structure itself collapses, since the frame wall thickness (FWT) of the M41S materials is lower and this may also contributes to the leaching of the vanadia species in a definite environment. These leached out vanadia species can interact with the water molecules present in the oxidant and can form well-homogenized different vanadium peroxo species [44], thus enhancing the oxidation of the organic substrates much faster as reaction progresses. Interestingly, XRD patterns of the V-MCM-41 materials after reaction shows a disappearance of the long-range ordered peak with a corresponding decrease in the a_0 values, pointing toward a unit cell contraction with the loss of heteroatoms from the framework positions.

4. Conclusion

In short, a series of vanadium-substituted, -grafted, and -immobilized mesoporous MCM-41 were synthesized and their surface property and activity differences were compared by various physicochemical techniques and catalytic evaluations. Contrary to earlier results, with the percentage of vanadia incorporation, well distinct XRD patterns with large pore sizes are observed for V-MCM-41 catalysts, while for the postsynthesis modified materials a decrease in structural ordering of the mesoporous support is observed after grafting/immobilization. Spectroscopic characterizations reveal that vanadium is incorporated into the framework positions for V-MCM-41 samples while the greater percentage of active species resides on the surface of V/MCM-41, enhancing the formation of higher coordinated vanadium species after calcination. Temperature-programmed reduction measurements show that vanadia species in V-MCM-41 are reduced at lower temperatures than the V/MCM-41 catalyst, thus pointing to the presence of isolated tetrahedral vanadyl sites on V-MCM-41 and "polymeric-like" vanadium species on the grafted catalyst. For the V-MCM-41 catalyst, since a greater portion of the vanadium species are well buried inside the pore channels of the mesoporous support they exist

as nonaccessible species for the reactant molecule while the formation of higher but dispersed surface vanadia species in the grafted catalyst may accounts for its enhanced activity behavior. The high catalytic performance of the immobilized catalysts may arise from active metal site isolation and hence favor an easy approach for the reactants to the active extraframework metal sites. However, the observed activity of the V-MCM-41 and V/MCM-41 catalyst is attributed to the presence of leached vanadia species and its interactions with H_2O_2 are highlighted with a series of experiments. Heterogenity studies show that the immobilized catalysts are more stable than the incorporated/grafted catalysts; as for the former the versatile coordination ability of the amino groups prevents the removal of vanadia species even during drastic reaction conditions and hence points and proves the novelty of anchored complex species for various oxidation reactions.

Acknowledgments

The authors are very grateful to (Drs.) Ramanathan, D. Srinivas, S.P. Mirajkar, Renu Parischa, N.E. Jacob, and N.R. Shiju for their kind assistance in the characterization of the catalysts and for useful discussions. S.S. thanks CSIR, India, for a junior research fellowship and task force project funded by CSIR (P23-CMM0005-B) for the financial assistance.

References

[1] Q. Zhang, Y. Wang, Y. Ohishi, T. Shishido, K. Takehira, J. Catal. 202 (2001) 308.
[2] H. Fujiyama, I. Kohara, K. Iwai, S. Nishiyama, S. Tsuruya, M. Masai, J. Catal. 188 (1999) 417.
[3] J. Evans, A.B. Zaki, M.Y. El-Sheikh, S.A. El-Safty, J. Phys. Chem. B 104 (2000) 10,271.
[4] W.A. Carvalho, M. Wallau, U. Schuchardt, J. Mol. Catal. A: Chem. 144 (1999) 91.
[5] J.S. Beck, J.C. Vartuli, W.J. Roth, M.E. Leonowicz, C.T. Kresge, K.D. Schmitt, C.T.-W. Chu, D.H. Olson, E.W. Sheppard, S.B. McCullen, J.B. Higgins, J.L. Schlenker, J. Am. Chem. Soc. 114 (1992) 10,834.
[6] J.S. Reddy, P. Liu, A. Sayari, Appl. Catal. A 148 (1996) 7.
[7] S.C. Laha, R. Kumar, Micropor. Mesopor. Mater. 53 (2002) 163.
[8] D. Wei, W.-T. Chuch, G.L. Haller, Catal. Today 51 (1999) 501.
[9] Z. Luan, J. Xu, H. He, J. Klinowski, L. Kevan, J. Phys. Chem. 100 (1996) 19,595.
[10] V. Parvulescu, B.L. Su, Catal. Today 69 (2001) 315.
[11] K. Lemke, H. Ehrich, U. Lohse, H. Berndt, K. Jahnisch, Appl. Catal. A 6401 (2003) 1.
[12] Y. Deng, C. Lettmann, W.F. Maier, Appl. Catal. A 214 (2001) 31.
[13] P. Wu, T. Tatsumi, T. Komatsu, T. Yashima, Chem. Mater. 14 (2002) 1657.
[14] C.-H. Lee, T.-S. Lin, C.-Y. Mou, J. Phys. Chem. B 107 (2003) 2543.
[15] D. Das, C.-M. Tsai, S. Cheng, Chem. Commun. (1999) 473.
[16] C.W. Lee, W.O. Lee, S.E. Park, Catal. Today 61 (2000) 137.
[17] Y. Deng, C. Lettmann, W.F. Maier, Appl. Catal. A 214 (2001) 31.
[18] K.M. Reddy, I. Moudrakovski, A. Sayari, J. Chem. Soc., Chem. Commun. (1994) 1059.
[19] T. Chirayil, P.Y. Zavalij, M.S. Whittingham, Chem. Mater. 10 (1998) 2629.
[20] V. Parvulescu, C. Dascalescu, B.L. Su, Stud. Surf. Sci. Catal. 135 (2001) 4772.
[21] N. Lang, P. Delichere, A. Tuel, Micropor. Mesopor. Mater. 56 (2002) 203.
[22] M.D. Alba, Z. Luan, J. Klinowski, J. Phys. Chem. 100 (1996) 2178.
[23] P. Van der Voort, M. Morey, G.D. Stucky, M. Mathieu, E.F. Vansant, J. Phys. Chem. B 102 (1998) 585.
[24] M. Baltes, K. Cassiers, P. Van der Voort, B.M. Weckhuysen, R.A. Schoonheydt, E.F. Vansant, J. Catal. 197 (2001) 160.
[25] A.B. Bourlinos, Th. Karakoatas, D. Petridis, J. Phys. Chem. B 107 (2003) 920.
[26] J.R. Sohn, Zeolites 6 (1986) 225.
[27] B.M. Reddy, I. Ganesh, B. Chowdary, Catal. Today 49 (1999) 115.
[28] M. Mathieu, P. Van der Voort, B.M. Weckhuysen, R.R. Rao, G. Catana, R.A. Schoonheydt, E.F. Vansant, J. Phys. Chem. B 105 (2001) 3393.
[29] M. Morey, A. Davidson, H. Eckert, G. Stucky, Chem. Mater. 8 (1996) 486.
[30] D.G. Barton, M. Shtein, R.D. Wilson, S.L. Soled, E. Iglesia, J. Phys. Chem. B 103 (1999) 630.
[31] H. So, M.T. Pope, Inorg. Chem. 11 (1972) 1441.
[32] B. Olthof, A. Khodakov, A.T. Bell, E. Iglesia, J. Phys. Chem. B 104 (2000) 1516.
[33] N. Krishnamachari, C. Calvo, Can. J. Chem. 49 (1971) 1629.
[34] H. Berndt, A. Martin, A. Bruckner, E. Schreier, D. Muller, H. Kosslick, G.U. Wolf, B. Lucke, J. Catal. 191 (2000) 384.
[35] G. Grubert, J. Rathousky, G.S. Ekloff, M. Wark, A. Zukal, Micropor. Mesopor. Mater. 22 (1998) 225.
[36] Z. Zhu, M. Hartmann, E.M. Maes, R.S. Czernuszewicz, L. Kevan, J. Phys. Chem. B 104 (2000) 4690.
[37] B. Solsona, T. Blasco, J.M. Lopez Nieto, M.L. Pena, F. Rey, A. Vidal-Moya, J. Catal. 203 (2001) 443.
[38] S.C. Laha, P. Mukherjee, S.R. Sainkar, R. Kumar, J. Catal. 207 (2002) 1.
[39] S. Shylesh, S. Sharma, S.P. Mirajkar, A.P. Singh, J. Mol. Catal. A: Chem. 212 (2004) 219.
[40] D. Margolese, J.A. Melero, S.C. Christiansen, B.F. Chmelka, G.D. Stucky, Chem. Mater. 12 (2000) 2448.
[41] A. Corma, P. Esteve, A. Martinez, J. Catal. 161 (1996) 11.
[42] H. Jing, Z. Guo, D.G. Evans, X. Duan, J. Catal. 212 (2002) 22.
[43] R.A. Sheldon, M. Wallau, I.W.C.E. Arends, U. Schuchardt, Acc. Chem. Res. 31 (1998) 485.
[44] H. Mimoun, L. Saussine, E. Daire, M. Postel, J. Fischer, R. Weiss, J. Am. Chem. Soc. 105 (1983) 3101.